nature structural & molecular biology

The elongation rate of RNA polymerase determines the fate of transcribed nucleosomes

Lacramioara Bintu[1,2,7,8], Marta Kopaczynska[3,7,8], Courtney Hodges[4,7], Lucyna Lubkowska[5], Mikhail Kashlev[5] & Carlos Bustamante[1–4,6]

Upon transcription, histones can either detach from DNA or transfer behind the polymerase through a process believed to involve template looping. The details governing nucleosomal fate during transcription are not well understood. Our atomic force microscopy images of yeast RNA polymerase II–nucleosome complexes confirm the presence of looped transcriptional intermediates and provide mechanistic insight into the histone-transfer process through the distribution of transcribed nucleosome positions. Notably, we find that a fraction of the transcribed nucleosomes are remodeled to hexasomes, and this fraction depends on the transcription elongation rate. A simple model involving the kinetic competition between transcription elongation, histone transfer and histone-histone dissociation quantitatively explains our observations and unifies them with results obtained from other polymerases. Factors affecting the relative magnitude of these processes provide the physical basis for nucleosomal fate during transcription and, therefore, for the regulation of gene expression.

DNA in eukaryotic cells is tightly wrapped into nucleosomes, which constitute a physical barrier for RNA polymerase II (Pol II) and function as important and ubiquitous regulators of transcription elongation[1–3]. *In vivo*, nucleosomes are disrupted to varying degrees by transcription elongation, with outcomes ranging from partial loss to complete removal and exchange of histones[4–9]. Because these different outcomes can influence further binding of chromatin remodeling factors and the advancement of subsequent transcribing polymerases on that gene[10], it is important to understand the mechanistic details that determine the fate of the nucleosome during transcription.

In vitro studies with the phage SP6 RNA polymerase and RNA polymerase III (Pol III) have shown that upon transcription, the histone octamer moves upstream by 40–95 base pairs (bp)[11–13]. Unexpectedly, later experiments suggested that transcription through a nucleosome by Pol II leads to H2A–H2B dimer loss and the formation of a hexamer whose position on DNA is unchanged[14,15]. Similar results were obtained with the *Escherichia coli* RNA polymerase[16]. This transfer process is believed to involve looping of the DNA template, but claims of template looping for Pol II have so far relied on indirect evidence[17–19]. Moreover, despite extensive work on characterizing the nucleosomal barrier[11–25], there is still little mechanistic understanding of how transcription dynamics affects histone turnover and little basis for rationalizing differences among polymerases.

Here we use atomic force microscopy (AFM) to obtain snapshots of individual Pol II–nucleosome complexes from *Saccharomyces cerevisiae* before, during and after transcription. These images allow us to directly visualize nucleosome integrity and position after transcription, to look for DNA looping during histone transfer, and to explore conditions that favor partial versus complete histone transfer.

RESULTS

Identification of transcribed complexes

Briefly, we assembled Pol II elongation complexes on a 96-bp DNA template[14,17] and ligated them to 574 bp of DNA containing a single nucleosome loaded on the 601 nucleosome positioning sequence (NPS)[26] (see Methods and **Supplementary Fig. 1**). We incubated these complexes either in the absence ('stalled sample', **Fig. 1a**) or presence ('chased sample', **Fig. 1b**) of nucleotide triphosphates (NTPs), fixed them with formaldehyde and imaged them using AFM (see Methods). Because Pol II has a considerably larger molecular weight (~550 kDa) than the nucleosome (~190 kDa), it is possible to unambiguously distinguish the two complexes by their different sizes in the images (**Fig. 1a–c**). We measured the lengths of the different segments of free DNA (that is, the DNA not covered by protein, **Fig. 1c**) as well as the heights of the proteins for complexes that have both the nucleosome and the polymerase[27] (see Methods).

[1]Jason L. Choy Laboratory of Single-Molecule Biophysics, University of California, Berkeley, Berkeley, California, USA. [2]Department of Physics, University of California, Berkeley, Berkeley, California, USA. [3]California Institute for Quantitative Biosciences, University of California, Berkeley, Berkeley, California, USA. [4]Biophysics Graduate Group, University of California, Berkeley, Berkeley, California, USA. [5]National Cancer Institute-Frederick, US National Institutes of Health, Center for Cancer Research, Frederick, Maryland, USA. [6]Howard Hughes Medical Institute, Department of Chemistry and Molecular & Cell Biology, University of California, Berkeley, Berkeley, California, USA. [7]Present addresses: Division of Biology, California Institute of Technology, Pasadena, California, USA (L.B.); Institute of Biomedical Engineering and Instrumentation, Wroclaw University of Technology, Wroclaw, Poland (M.K.); Department of Pathology, Stanford University School of Medicine, Stanford, California, USA (C.H.). [8]These authors contributed equally to this work. Correspondence should be addressed to C.B. (carlos@alice.berkeley.edu).

Received 28 April; accepted 13 September; published online 13 November 2011; doi:10.1038/nsmb.2164

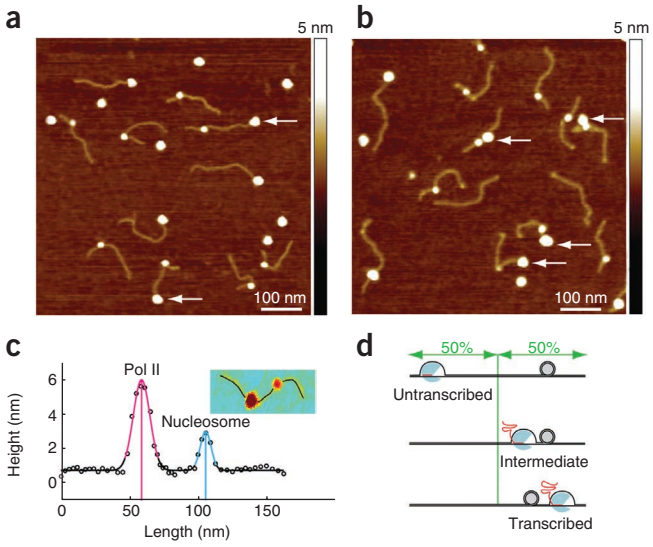

Figure 1 Snapshots of transcription. (**a**,**b**) AFM images of stalled (**a**, no NTPs added) and chased (**b**, all four NTPs added) complexes. Only complexes that contain both the polymerase and nucleosome are included for analysis (unless otherwise specified); white arrows indicate Pol II in these complexes. (**c**) The height profile of an example complex (inset) is plotted along the DNA path as black circles. The Pol II and nucleosome heights are fitted to Gaussian curves shown in magenta and blue, respectively. The free DNA segment lengths (black part of the fitted curve) are defined as the lengths of the paths that start two s.d. away from the centers of the proteins. (**d**) Schematic of the algorithm used to identify the Pol II–nucleosome complexes. When Pol II (blue) is on the long arm of the nucleosome (gray) and its center has not yet reached the middle of the DNA template (green vertical line), we tag the complex as untranscribed. When Pol II has passed the middle line of the template, and the Pol II and nucleosome edges are within 5 nm or less of each other, we tag the complexes as intermediate. When Pol II is on the short arm of the nucleosome, we tag the complex as transcribed.

The position of the polymerase in stalled samples was centered at the start site of transcription (**Fig. 1a** and **Supplementary Fig. 2a**). By contrast, after addition of all four nucleotides, Pol II was distributed along the entire length of the DNA template, indicating that transcription had ensued (**Fig. 1b** and **Supplementary Fig. 2b**).

To determine which complexes in the chased sample had completed transcription through the nucleosome, we made use of the fact that the DNA upstream of the nucleosome, containing the start site of Pol II, was about three times longer than the DNA downstream of the nucleosome. When Pol II was on the long arm and did not contact the nucleosome, we reasoned that transcription had not yet proceeded into the nucleosomal region, and we labeled these nucleosomes as 'untranscribed'. Conversely, when Pol II was on the short arm, we inferred that transcription through the nucleosome was completed, and we labeled these nucleosomes 'transcribed' (**Fig. 1d** and **Supplementary Fig. 2b**). In order to correctly identify transcribed nucleosomes, we assumed that even if their positions changed from the original NPS, they remained on the same half of DNA after transcription. We used a boot-strapping method to check this assumption: if the nucleosome moved on the other half of the DNA, we would expect a change in the position distribution of nucleosomes that were untranscribed. However, for complexes identified as untranscribed in the chased sample, the position of the nucleosome is unchanged compared to untranscribed nucleosomes imaged in the absence of Pol II (**Fig. 2a**, $P = 0.3$, t-test), indicating that our identification of these nucleosomes as untranscribed is valid.

Nucleosome position after transcription

In order to get an accurate measurement of the changes in position of the nucleosomes (see Methods, **Supplementary Discussion** subsection 1 and **Supplementary Table 1**), we compared the length of the free DNA segment upstream of transcribed nucleosomes (**Fig. 2b**, red) to that of untranscribed nucleosomes from a sample without Pol II (**Fig. 2b**, blue). The distribution for transcribed nucleosomes is broader, and there is a modest but statistically significant shift to shorter lengths (6 nm, $P = 5 \times 10^{-8}$, t-test). The partial overlap with the corresponding distribution of untranscribed nucleosomes suggests that the majority of the nucleosomes were placed at the same location after transcription, in accordance with previously published results[14]. However, our single-molecule method, used in conjunction with a DNA sequence that positioned the nucleosome uniquely, allows us to observe that a small subpopulation of the transcribed nucleosomes (approximately 20%) moved immediately upstream of their original position by 24 nm (72 bp), on average (**Fig. 2b**). This upstream relocation of the histones suggests a looping mechanism of histone transfer, a mechanism initially proposed for the phage polymerase[11,21] and, more recently, for Pol II[17].

DNA looping during histone transfer

In models of DNA looping during nucleosomal transcription, the histones from a partially unwrapped nucleosome situated downstream of the transcribing polymerase are assumed to simultaneously contact a DNA segment upstream of the polymerase, forming a loop. According to such models, this process eventually leads to the transfer of histones behind the polymerase and permits transcription to resume. In agreement with this idea, we found many intermediate complexes in which Pol II was in the process of transcribing the nucleosome that showed the histones contacting the DNA segments both upstream and downstream of Pol II (**Fig. 3a**).

The distribution of total free DNA lengths for intermediate complexes in which Pol II was in the process of transcribing the nucleosome is different from that of complexes where Pol II had started transcribing but had not yet reached the nucleosome ($P = 0.009$, Kolmogorov-Smirnov test; see **Supplementary Fig. 2** for populations selected). Because the free-DNA–length distribution for these intermediate complexes was not well described by a single Gaussian ($P = 0.03$, Lilliefors test), we fit this distribution with two Gaussians (**Fig. 3b**). The main peak is identical with the corresponding distribution for complexes in which Pol II had started transcribing

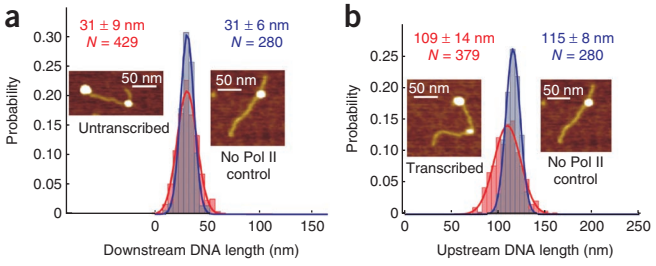

Figure 2 Nucleosome position. (**a**) The length of the downstream free DNA segments for untranscribed nucleosomes (red) and complexes without Pol II (blue). (**b**) The length of the upstream free DNA segment for transcribed nucleosomes (red) and complexes without Pol II (blue). Mean and s.d. for N polymerase–nucleosome complexes are indicated in each case.

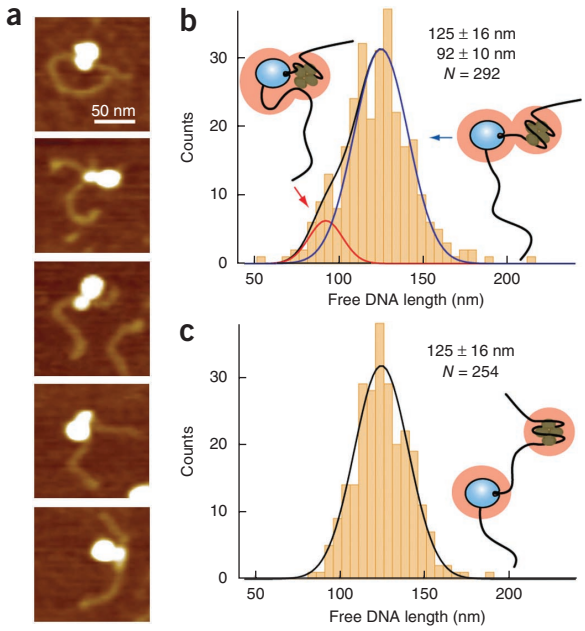

Figure 3 DNA looping during histone transfer. (**a**) AFM images of complexes in which the histones contact both the upstream and downstream DNA. (**b**) Free DNA length in the presence of NTPs (all concentrations) in complexes where Pol II is in the process of transcribing the nucleosome (the length of DNA between Pol II and the nucleosome is less than 5 nm apart). (**c**) Complexes where Pol II has started transcription but has not yet reached the nucleosome. Insets show the presumed structures of each population, with Pol II in blue, the DNA in black and the histones in brown; the pink shading reflects the apparent broadening of the molecules due to the geometry and size of the AFM tip. Mean and s.d. of the total free DNA lengths (*N*) are indicated.

but had not yet reached the nucleosome (**Fig. 3c**). The second peak corresponds to an additional population of intermediates in which the DNA outside the polymerase–nucleosome complex was shorter by ~30 nm. We interpret this shortening as evidence that the template in the proximity of the nucleosome participates in a loop that facilitates histone transfer behind the polymerase, a loop that cannot be resolved because of the broadening effect of the AFM tip (**Fig. 3b**, inset). The estimated size of these DNA loops (~90 bp) is smaller than the persistence length of DNA (~150 bp), and they may be facilitated by the putative 90° bend that Pol II introduces into its DNA template[18,19,28,29].

Pol II transcription produces hexamers and octamers

As Pol II advances onto the nucleosomal template, the DNA detaches from the core histones, exposing them to the surrounding conditions. Because the octamer consists of a collection of positively charged histones, it is unstable at salt concentrations under 1 M[30,31]. Thus, unless the core histones contact another piece of DNA that can neutralize their charges and stabilize their association, the octamer may dissociate with partial loss of its components. Indeed, loss of an H2A–H2B dimer and the formation of a hexasome upon transcription by Pol II has been reported[14,15]. Consistent with these results, we observed a reduction in the apparent physical size of transcribed nucleosomes (**Fig. 4a**). Moreover, the heights of these complexes consisted of two populations: one similar to untranscribed nucleosomes (3 ± 0.4 nm, **Fig. 4b**) and the other corresponding to subnucleosomal particles with lower height (2.1 ± 0.3 nm, **Fig. 4c**).

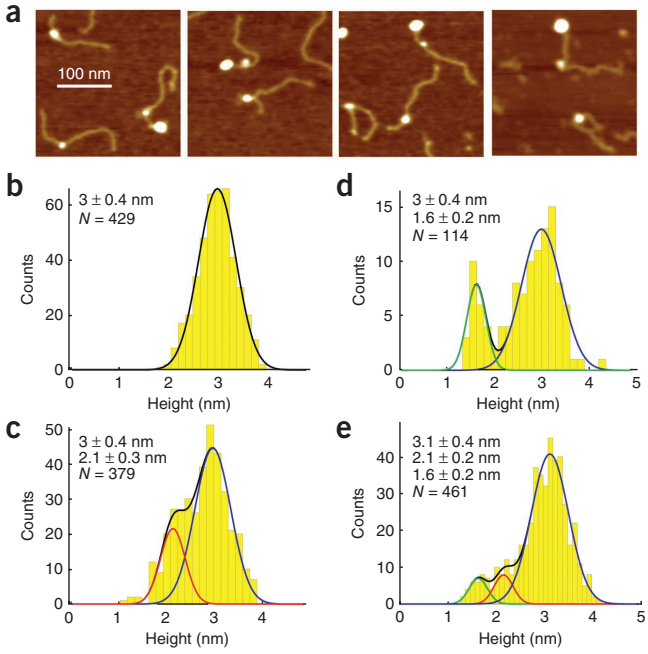

In order to identify the transcribed particles with decreased height, we reconstituted and imaged histone tetramers on DNA using the same methods as for octamers[32], except with H2A and H2B histones omitted. The height of the tetramers, 1.6 ± 0.2 nm, was substantially lower than that of the transcribed particle, 2.1 ± 0.3 nm (**Fig. 4d**). Moreover, when we destabilized complete octameric nucleosomes by incubating them in 1 M KCl, we obtained three nucleosomal species, consistent with what is expected of octamers, hexamers and tetramers (**Fig. 4e**). The heights of the middle peak, which we identified as a population of hexamers, matched the heights of the subnucleosomal particles resulting from transcription.

Hexamer-to-octamer ratio depends on the elongation rate

Most notably, we found that the fraction of smaller subnucleosomal particles observed after transcription depended on the rate of elongation. When transcription was carried out at low NTP concentration (100 μM), only 10 ± 3% of the transcribed nucleosomes were converted to hexasomes (**Fig. 5a**). Increasing the NTP concentration to 200 μM augmented the percentage of hexasomes to 17 ± 3% (**Fig. 5b**). At saturating NTP conditions (1,000 μM), 25 ± 5% of the transcribed nucleosomes were converted to hexasomes (**Fig. 5c**). No changes were observed in the sizes of untranscribed nucleosomes in these samples (**Fig. 5d–f**).

We attribute these different outcomes of transcription to the kinetic competition between histone dissociation from a partially

Figure 4 Transcription leads to hexamer formation. (**a**) Images illustrating nucleosome changes upon transcription. The nucleosomes with reduced height are shown next to normal-sized nucleosomes for comparison. (**b**,**c**) Histograms of nucleosome heights for untranscribed (**b**) and transcribed (**c**) nucleosomes at all NTP concentrations show the appearance of subnucleosomal particles with reduced height (fit by the red curve). (**d**) Heights of octamers (fit by the blue curve) compared with tetramers (fit by the green curve). (**e**) Height of nucleosomes destabilized by incubation in a high-salt solution (1 M KCl). We identify the three peaks as tetramers (green), hexamers (red) and octamers (blue). Mean and s.d. for *N* complexes are indicated in each case.

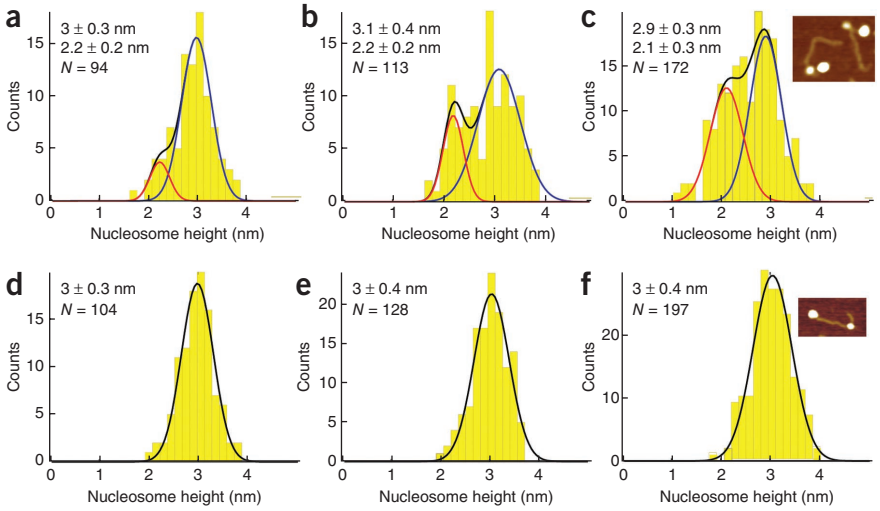

Figure 5 Histone transfer outcome depends on the speed of transcription. (**a**–**c**) Nucleosome heights for molecules in which Pol II passed the nucleosome, in solutions containing 100 μM NTPs (**a**), 200 μM NTPs (**b**) and 1,000 μM NTPs (**c**). (**d**–**f**) Nucleosome heights for molecules where Pol II has not passed the nucleosome, in solutions containing 100 μM NTPs (**d**), 200 μM NTPs (**e**) and 1,000 μM NTPs (**f**). The continuous curves represent Gaussian fits to the data. Insets show transcribed nucleosomes (top) and untranscribed nucleosomes (bottom). Mean and s.d. for *N* complexes are indicated in each case.

unwrapped nucleosome and histone transfer to the upstream DNA. Initially, as the nucleosome partially unwraps during Pol II advancement, enough of the histone core is exposed to allow contact with the upstream DNA through a temporary DNA loop, but not so much as to cause H2A–H2B dissociation. During slow transcription (100 μM NTPs) this partially exposed histone intermediate lasts long enough to allow transfer of the intact octamer onto the upstream DNA. However, if the rate of transcription increases slightly, more of the nucleosome unwraps, and as enough of the histone core becomes exposed, dimer dissociation starts competing with octamer transfer to the upstream DNA. Under these conditions, representative of transcription at 200 μM and 1,000 μM NTPs, both octamers and hexamers can be found as a result of transcription. Finally, when the rates of transcription are even higher, enough DNA unwraps from the surface of the histone core that the complete histone detachment from DNA greatly outcompetes the rates of histone transfer and histone-histone dissociation, thus leading to bare DNA formation.

Elongation, looping and histone dissociation compete

The dependence of the outcome of transcription on the speed of elongation indicates that a kinetic competition exists between the net rate of nucleosome unwrapping during elongation (k_{ue}), octamer transfer (k_t) and dimer dissociation (k_d) during transcription through the nucleosome (**Fig. 6a**).

In this competition model, the probability of observing a hexamer (P_{hex}), an octamer (P_{oct}) or bare DNA (P_{bare}) after transcription can be written as

$$P_{hex} = \left(\frac{k_{ue}}{k_t + k_{ue}}\right)^N \left(\frac{k_d}{k_t + k_d} + \frac{k_t}{k_t + k_d} \times \left(\frac{k_{ue}}{k_t + k_{ue} + k_d}\right)^{N_T - N}\right) - \left(\frac{k_{ue}}{k_t + k_{ue}}\right)^{N_T}$$

$$P_{oct} = 1 - \left(\frac{k_{ue}}{k_t + k_{ue}}\right)^N \left(\frac{k_d}{k_t + k_d} + \frac{k_t}{k_t + k_d} \times \left(\frac{k_{ue}}{k_t + k_{ue} + k_d}\right)^{N_T - N}\right)$$

$$P_{bare} = \left(\frac{k_{ue}}{k_{ue} + k_t}\right)^{N_T}$$

where N is the number of unwrapped base pairs that allow octamer transfer but not dimer dissociation, and where we assume the competition happens at every base transcribed, along the entire length of the nucleosome, which contains a total number $N_T = 147$ base pairs of wrapped DNA[33] (see **Supplementary Discussion** subsection 2 for derivation). The model described here predicts that as the overall elongation rate through the nucleosome (k_{ue}) becomes larger, the probability of complete histone removal and the resulting production of bare DNA (P_{bare}) should increase monotonically, whereas the production of transferred octamers (P_{oct}) should decrease monotonically. Notably, this model predicts that the probability of hexamer formation should increase from low to moderate Pol II elongation rates, because as the rate of elongation-dependent octamer unwrapping increases, the probability of histone dissociation effectively competes with that of octamer transfer, enhancing the production of hexamers, as observed in our study (first term in P_{hex} dominates). However, as the rate of elongation and nucleosome unwrapping increases further, the rate of histone dissociation is outcompeted by the rate of complete histone removal, and the production of hexamers should attain a maximum and eventually decrease (the last term in P_{hex} dominates).

To test this model, we sought to determine the rates involved in this process. We found that the net rate of nucleosome unwrapping during elongation was equal to the average overall velocity of transcription through the nucleosome (including pausing due to backtracking), which at saturating NTP concentrations (1,000 μM) is k_{ue} = 1 bp s^{-1} (ref. 17). Using the Michaelis-Menten constant for NTP hydrolysis, which we measured to be K_m =100 μM (**Supplementary Fig. 3** and **Supplementary Discussion** subsection 3), we estimated the net rates of transcription through the nucleosome at 200 μM and 100 μM NTPs to be about 0.7 bp s^{-1} and 0.5 bp s^{-1}, respectively. Finally, to determine the rate of H2A–H2B dimer loss for preassembled octamers directly exposed to the salt concentration used in these studies (300 mM KCl), we carried out an ensemble FRET-based assay with fluorescently labeled H2B and H4 (ref. 31). These experiments gave $k_d = 0.027 \pm 0.001$ s^{-1} (**Supplementary Fig. 4** and **Supplementary Discussion** subsection 4).

Our fit of the experimental data (**Fig. 6b**) shows that this simple competition model correctly captures the details of hexamer and octamer transfer probabilities, as well as that of complete histone removal, when the initial DNA unwrapped region allowing only octamer transfer (but no dimer dissociation) is set to $N = 40 \pm 5$ bp and the rate of histone transfer is set to $k_t = 0.02 \pm 0.005$ s^{-1}. Notice that the value of N we obtained is consistent with the amount of DNA contacted by the H2A–H2B dimer (~30 bp[33]). Therefore, we predict that histone or DNA modifications that destabilize the wrapping of this 40-bp region would favor hexamer formation. The rate of histone transfer is slow and similar to that of dimer dissociation. For histone transfer, the rate-limiting process is most likely the actual handoff

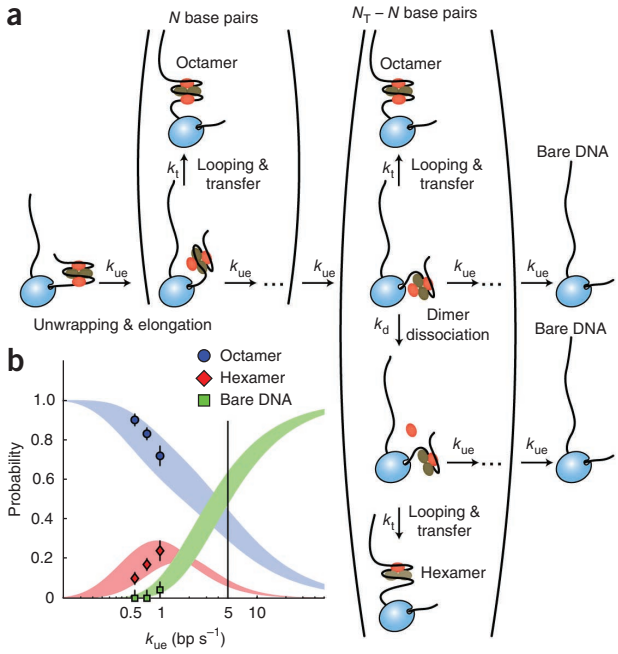

Figure 6 Histone transfer model. (**a**) Kinetic scheme of transcription and histone transfer. Pol II is shown in blue, H2A–H2B dimers in red, H3–H4 dimers in brown and DNA in black. (**b**) Hexamer (red) and octamer (blue) transfer probabilities, as well as bare DNA formation (green) are plotted as a function of the net nucleosome unwrapping rate during elongation (k_{ue}). Experimental data are shown as circles; the shaded areas represent the model predictions, with the width reflecting uncertainties in k_t and N, as indicated in the text. The vertical black line marks the elongation rate for the faster polymerase Pol III. The errors represent the s.d. among three different sample preparations.

of the histones from the downstream to the upstream DNA, because looping that results from DNA-bending fluctuations is known to be much faster[34].

Our mathematical model of histone transfer takes into consideration the increased probability of pausing due to backtracking at low NTP concentrations and the effect of this pausing on the overall transcription rate (**Supplementary Discussion** subsection 3). However, in addition to slowing down the overall elongation rates, extensive backtracking may allow the upstream DNA to rotate so as to face toward the unwrapped histone core, facilitating histone transfer further[18].

DISCUSSION

Our results support a model where nucleosome unwrapping during elongation exposes the histones so that they dissociate from the core octamer unless they interact with another segment of DNA. We propose that because Pol II sharply bends the DNA, it positions the exposed histones very close to the DNA immediately upstream of the polymerase, thus mediating histone transfer to the same DNA molecule through looping. This positioning hypothesis has been proposed before[18,19] and explains both the small size of the loops that allow histone transfer by bridging upstream and downstream DNA and the small upstream shift in the position of transcribed nucleosomes. Our observation that only a minority of nucleosomes changed position after transcription may have been influenced by our use of a strong NPS, which could have biased the histones to transfer and rewrap at the same location as before transcription. In addition, the total percentage of shifted nucleosomal particles (hexamers and octamers together) decreased slightly as the NTP concentration was lowered (**Supplementary Table 2**). Presumably, at lower NTP concentrations, the slower transcription is more likely to allow the histones to equilibrate on their original position during rewrapping.

In this model of nucleosomal transcription, faster transcription leads to faster overall nucleosome unwrapping, favoring histone dissociation. However, other factors affecting the rewrapping of the histones could influence the outcome of the competition. For example, a trailing polymerase blocking access of the unwrapped histones to upstream DNA[15,35] and histone mutations that destabilize histone-DNA wrapping[36] have both been shown to inhibit histone transfer and to promote histone dissociation *in vitro*, as our model predicts.

Our competition model also explains why faster polymerases produce a mix of octamers and bare DNA but yield little or no hexamers upon transcription. For instance, *in vitro,* the majority of Pol III complexes in our study completed transcription through a nucleosome in approximately 30 s (ref. 12) (**Fig. 6b**, vertical black line), so we predict that octamer transfer is likely to be approximately 40%, whereas bare DNA production should be about 50%. To obtain hexasomes, on the other hand, two slow processes have to occur before Pol III can finish transcription: dimer dissociation and histone transfer, making the probability of hexamer transfer very unlikely—about 10%—under these fast transcription conditions. Note that in this model, we only consider histone transfer within the same DNA molecule and do not include the probability of histone rebinding to other DNA molecules after complete dissociation. These predictions match previous experimental studies with Pol III reporting ~50% octamers and ~50% bare DNA[12] in the presence of competitor DNA, when only transfer in *cis* was measured.

Moreover, *in vitro* transcription by the even faster SP6 polymerase also leads to the formation of octamers and bare DNA, without hexamer formation, with the percentage of bare DNA increasing as the speed of elongation is increased[11]. We estimate that SP6 RNAP is faster than 5 bp s^{-1}, so our model predicts that the outcome of transcription should be dominated by bare DNA. This prediction might at first seem to contradict the experimental results, in which much lower levels of bare DNA have been observed, especially in the absence of competitor DNA[11]. However, our model only considers transfer of the histones in *cis* (within the same DNA molecule). Although this is the prevalent scenario for Pol II, we believe that for faster polymerases (such as SP6), much of the histone transfer happens in *trans*. Because Pol II moves more slowly, the histones have time to equilibrate with the DNA upstream (which is at a higher local concentration than other pieces of DNA). By contrast, for faster polymerases, the histone octamer detaches quickly, and because it is floating freely in solution, it is now just as likely to bind to any piece of DNA (in *cis* or in *trans*). This interpretation is supported by work showing that for the SP6 polymerase, adding competitor DNA to the reaction increases the amount of bare transcribed DNA[11]. Moreover, it appears that transfer in *trans* is seen at higher NTP concentrations, whereas transfer in *cis* dominates at lower NTP concentrations, in agreement with our model. However, it is difficult to quantitatively compare these predictions to data obtained for the SP6 RNAP, as there are multiple—and unknown—transcription rounds for each DNA molecule, leading to a higher probability for complete histone dissociation than is predicted by our model. In addition, we propose that the geometry of the elongation complex influences histone transfer, so we expect that polymerases having substantially different sizes and structures could lead to different position distributions and transfer probabilities for the transcribed nucleosomes. The magnitude of these effects remains to be tested.

Gene regulation *in vivo* may result from the modification of any one of the competing rates involved in elongation on a nucleosomal template. Although we used a DNA sequence with a higher affinity

for the nucleosome than other naturally occurring sequences, we predict that transcription through a weaker nucleosome will be faster (k_{ue} rate is increased because there is a higher probability of finding the nucleosome locally unwrapped[17]), and the transfer probability will decrease (because of lowered rewrapping rates of histones to the upstream DNA). Both these effects would result in a higher percentage of bare DNA and hexasome formations after transcription of weaker positioning sequences. More notably, elongation factors that increase the net transcription rate of Pol II through the nucleosome would result in an increased chance of complete histone removal from DNA. Alternatively, dimer dissociation from the partially unwrapped octamer could be faster for certain histone variants of H2A[37] or in the presence of histone chaperones that bind the dimer, increasing the likelihood of hexasome formation, as has been shown *in vitro*[38]. Such transcription-induced alterations in chromatin structure may affect gene expression *in vivo* by reducing or eliminating nucleosomal barriers for future transcription elongation events in a similar manner to results obtained *in vitro*[15,18], or by altering the accessibility of transcription factor binding sites[39]. Finally, we point out that the findings communicated here might also be relevant to other processes that involve the advancement of molecular motors on DNA wrapped in nucleosomes, such as processive DNA replication and chromatin remodeling[40].

METHODS

Methods and any associated references are available in the online version of the paper at http://www.nature.com/nsmb/.

Note: Supplementary information is available on the Nature Structural & Molecular Biology website.

ACKNOWLEDGMENTS

We thank M. Dangkulwanich, T. Ishibashi, B. Onoa, P. Visperas and Y. Wu for experimental assistance and helpful discussions, and C. Rivetti for sharing the ALEX code. This work was supported by the Howard Hughes Medical Institute and by US National Institutes of Health grant R01-GM032543-30 (to C.B.).

AUTHOR CONTRIBUTIONS

L.B., M.Kopaczynska, C.H. and C.B. designed the research. M.Kopaczynska, L.B. and C.H. prepared materials and conducted experiments. L.B. and M.Kopaczynska analyzed the data. L.L. and M.Kashlev contributed materials and discussed the manuscript. L.B., M.Kopaczynska, C.H. and C.B. wrote the paper.

COMPETING FINANCIAL INTERESTS

The authors declare no competing financial interests.

Published online at http://www.nature.com/nsmb/.
Reprints and permissions information is available online at http://www.nature.com/reprints/index.html.

1. Churchman, L.S. & Weissman, J.S. Nascent transcript sequencing visualizes transcription at nucleotide resolution. *Nature* **469**, 368–373 (2011).
2. Subtil-Rodríguez, A. & Reyes, J.C. BRG1 helps RNA polymerase II to overcome a nucleosomal barrier during elongation, *in vivo*. *EMBO Rep.* **11**, 751–757 (2010).
3. Gaykalova, D.A. *et al.* A polar barrier to transcription can be circumvented by remodeler-induced nucleosome translocation. *Nucleic Acids Res.* **39**, 3520–3528 (2011).
4. Thiriet, C. & Hayes, J.J. Replication-independent core histone dynamics at transcriptionally active loci *in vivo*. *Genes Dev.* **19**, 677–682 (2005).
5. Thiriet, C. & Hayes, J.J. Histone dynamics during transcription: exchange of H2A/H2B dimers and H3/H4 tetramers during pol II elongation. *Results Probl. Cell Differ.* **41**, 77–90 (2006).
6. Dion, M.F. *et al.* Dynamics of replication-independent histone turnover in budding yeast. *Science* **315**, 1405–1408 (2007).
7. Kimura, H. & Cook, P.R. Kinetics of core histones in living human cells little exchange of H3 and H4 and some rapid exchange of H2B. *J. Cell Biol.* **153**, 1341–1353 (2001).
8. Schwabish, M.A. & Struhl, K. Asf1 mediates histone eviction and deposition during elongation by RNA polymerase II. *Mol. Cell* **22**, 415–422 (2006).
9. Jamai, A., Imoberdorf, R.M. & Strubin, M. Continuous histone H2B and transcription-dependent histone H3 exchange in yeast cells outside of replication. *Mol. Cell* **25**, 345–355 (2007).
10. Workman, J.L. Nucleosome displacement in transcription. *Genes Dev.* **20**, 2009–2017 (2006).
11. Studitsky, V.M., Clark, D.J. & Felsenfeld, G. A histone octamer can step around a transcribing polymerase without leaving the template. *Cell* **76**, 371–382 (1994).
12. Studitsky, V.M., Kassavetis, G.A., Geiduschek, E.P. & Felsenfeld, G. Mechanism of transcription through the nucleosome by eukaryotic RNA polymerase. *Science* **278**, 1960–1963 (1997).
13. Clark, D.J. & Felsenfeld, G. A nucleosome core is transferred out of the path of a transcribing polymerase. *Cell* **71**, 11–22 (1992).
14. Kireeva, M.L. *et al.* Nucleosome remodeling induced by RNA polymerase II loss of the H2A–H2B dimer during transcription. *Mol. Cell* **9**, 541–552 (2002).
15. Kulaeva, O.I., Hsieh, F.K. & Studitsky, V.M. RNA polymerase complexes cooperate to relieve the nucleosomal barrier and evict histones. *Proc. Natl. Acad. Sci. USA* **107**, 11325–11330 (2010).
16. Walter, W., Kireeva, M.L., Studitsky, V.M. & Kashlev, M. Bacterial polymerase and yeast polymerase II use similar mechanisms for transcription through nucleosomes. *J. Biol. Chem.* **278**, 36148–36156 (2003).
17. Hodges, C., Bintu, L., Lubkowska, L., Kashlev, M. & Bustamante, C. Nucleosomal fluctuations govern the transcription dynamics of RNA polymerase II. *Science* **325**, 626–628 (2009).
18. Kulaeva, O.I. *et al.* Mechanism of chromatin remodeling and recovery during passage of RNA polymerase II. *Nat. Struct. Mol. Biol.* **16**, 1272–1278 (2009).
19. Kulaeva, O.I. & Studitsky, V.M. Mechanism of histone survival during transcription by RNA polymerase II. *Transcr.* **1**, 85–88 (2010).
20. Izban, M.G. & Luse, D.S. Transcription on nucleosomal templates by RNA polymerase II *in vitro*: inhibition of elongation with enhancement of sequence-specific pausing. *Genes Dev.* **5**, 683–696 (1991).
21. Bednar, J., Studitsky, V.M., Grigoryev, S.A., Felsenfeld, G. & Woodcock, C.L. The nature of the nucleosomal barrier to transcription direct observation of paused intermediates by electron cryomicroscopy. *Mol. Cell* **4**, 377–386 (1999).
22. Walter, W. & Studitsky, V.M. Facilitated transcription through the nucleosome at high ionic strength occurs via a histone octamer transfer mechanism. *J. Biol. Chem.* **276**, 29104–29110 (2001).
23. Kireeva, M.L. *et al.* Nature of the nucleosomal barrier to RNA polymerase II. *Mol. Cell* **18**, 97–108 (2005).
24. Bondarenko, V.A. *et al.* Nucleosomes can form a polar barrier to transcript elongation by RNA polymerase II. *Mol. Cell* **24**, 469–479 (2006).
25. Luse, D.S., Spangler, L.C. & Újvári, A. Efficient and rapid nucleosome traversal by RNA polymerase II depends on a combination of transcript elongation factors. *J. Biol. Chem.* **286**, 6040–6048 (2011).
26. Lowary, P.T. & Widom, J. New DNA sequence rules for high affinity binding to histone octamer and sequence-directed nucleosome positioning. *J. Mol. Biol.* **276**, 19–42 (1998).
27. Rivetti, C. & Codeluppi, S. Accurate length determination of DNA molecules visualized by atomic force microscopy: evidence for a partial B- to A-form transition on mica. *Ultramicroscopy* **87**, 55–66 (2001).
28. Gnatt, A.L., Cramer, P., Fu, J., Bushnell, D.A. & Kornberg, R.D. Structural basis of transcription: an RNA polymerase II elongation complex at 3.3 A resolution. *Science* **292**, 1876–1882 (2001).
29. Cramer, P., Bushnell, D.A. & Kornberg, R.D. Structural basis of transcription: RNA polymerase II at 2.8 angstrom resolution. *Science* **292**, 1863–1876 (2001).
30. Eickbush, T.H. & Moudrianakis, E.N. The histone core complex: an octamer assembled by two sets of protein-protein interactions. *Biochemistry* **17**, 4955–4964 (1978).
31. Park, Y.J., Dyer, P.N., Tremethick, D.J. & Luger, K. A new fluorescence resonance energy transfer approach demonstrates that the histone variant H2AZ stabilizes the histone octamer within the nucleosome. *J. Biol. Chem.* **279**, 24274–24282 (2004).
32. Wittmeyer, J., Saha, A. & Cairns, B. DNA translocation and nucleosome remodeling assays by the RSC chromatin remodeling complex. *Methods Enzymol.* **377**, 322–343 (2004).
33. Luger, K., Mäder, A.W., Richmond, R.K., Sargent, D.F. & Richmond, T.J. Crystal structure of the nucleosome core particle at 2.8 Å resolution. *Nature* **389**, 251–260 (1997).
34. Huang, J., Schlick, T. & Vologodskii, A. Dynamics of site juxtaposition in supercoiled DNA. *Proc. Natl. Acad. Sci. USA* **98**, 968–973 (2001).
35. Jin, J. *et al.* Synergqstic action of RNA polymerases in overcoming the nucleosomal barrier. *Nat. Struct. Mol. Biol.* **17**, 745–752 (2010).
36. Hsieh, F.K., Fisher, M., Újvári, A., Studitsky, V.M. & Luse, D.S. Histone Sin mutations promote nucleosome traversal and histone displacement by RNA polymerase II. *EMBO Rep.* **11**, 705–710 (2010).
37. Bao, Y. *et al.* Nucleosomes containing the histone variant H2A.Bbd organize only 118 base pairs of DNA. *EMBO J.* **23**, 3314–3324 (2004).
38. Belotserkovskaya, R. *et al.* FACT facilitates transcription-dependent nucleosome alteration. *Science* **301**, 1090–1093 (2003).
39. Hayes, J.J. & Wolffe, A.P. Histones H2A/H2B inhibit the interaction of transcription factor IIIA with the *Xenopus borealis* somatic 5S RNA gene in a nucleosome. *Proc. Natl. Acad. Sci. USA* **89**, 1229–1233 (1992).
40. Bruno, M. *et al.* Histone H2A/H2B dimer exchange by ATP-dependent chromatin remodeling activities. *Mol. Cell* **12**, 1599–1606 (2003).

ONLINE METHODS

Proteins and DNA purification. His-tagged RNA polymerase II (*S. cerevisiae*, unphosphorylated C-terminal domain) was purified as previously described[41]. The 574-bp DNA template was prepared by PCR from a modified pUC19 plasmid[42] containing the 601 nucleosome positioning sequence[26]. Octamers were reconstituted from recombinant yeast histones[32] and loaded onto the template DNA using salt dialysis[43].

Assembly of elongation complexes with nucleosomes. Pol II was assembled on DNA using the same method and sequences as previously described[17], and the resulting elongation complexes were ligated to downstream DNA containing a preloaded nucleosome (**Supplementary Fig. 1**). The assembly and ligation were carried out in TB40 (20 mM HEPES, pH 7.8, 40 mM KCl, 10 mM $MgCl_2$, 10 μM $ZnCl_2$, 1 mM β-mercaptoethanol). Transcription was carried out at 25 °C in TB300 (which has the same composition as TB40, except with 300 mM KCl), using 1 mM of each NTP—unless otherwise specified—and 1 μM pyrophosphate, for 30 min.

In the sample used for calculating the position of untranscribed nucleosomes (**Fig. 2**, blue), the 93-bp double-stranded DNA (Integrated DNA Technologies) was ligated in excess to the 574-bp nucleosomal DNA, in the absence of Pol II.

Sample preparation for AFM and imaging. Following transcription, samples were fixed by incubating them with 1% (w/v) formaldehyde for 2 h at 25 °C. We removed the formaldehyde by dialyzing them in TB40 for 45 min at 25 °C For deposition, the samples were diluted in TB40 to a 2-nM DNA concentration, placed on freshly cleaved ultraclean mica (Grade V, Ted Pella), and incubated at room temperature for about 2 min. The mica discs were then rinsed with purified 18.2-MΩ deionized water and dried using a gentle N_2 gas flow, perpendicular to the mica surface.

AFM measurements were taken with a MultiMode NanoScope V atomic force microscope (Veeco Instruments) equipped with a type E scanner (vertical range of 10 μm × 10 μm × 2.5 μm). The samples were imaged in tapping mode using a commercial silicon cantilever (Nanosensors), with a high-resonance frequency in the range of 260–410 kHz and a spring constant of 46 N m^{-1}. Images (512 × 512 pixels) were captured in the trace direction, at a scan size of 1.5 μm, with a scan rate of 1.5 Hz. The imaging amplitude (amplitude set point) of the cantilever was maintained by the feedback circuitry to 80–85% of the free oscillation amplitude, and the scan angle was maintained at zero. All samples were measured at room temperature in air, at a relative humidity of 30%.

Image analysis. Image processing and data analysis were carried out using Matlab (MathWorks), with custom-written code based on ALEX[27,44]. We imported the images into Matlab, automatically masked all the points higher than 9 nm and flattened the images by subtracting from each line a polynomial of degree 2 that was fit to that line. We then identified all the objects higher than 0.2 nm in this flattened image, used those points as a mask, and generated each new line by removing the masked points and fitting the original line with a polynomial of degree 4.

For each complex, the DNA path (passing through the proteins) was digitized and fit by a polynomial of degree 3 (ref. 44). The polymerase and nucleosome center positions were recorded as the centers of the highest and second-highest Gaussian distributions, respectively, along the identified DNA path (**Fig. 1c**). The nucleosome heights were measured as the maximum height in a 4-nm box centered at the position of the nucleosome, to correct for cases when the DNA path does not pass through the center of the nucleosome. To account for small height variation among different depositions, we corrected the height of transcribed nucleosomes using the height of untranscribed nucleosomes as a standard. In the chased samples, we first identified the molecules that had Pol II but where Pol II had not yet crossed the nucleosome (as shown in **Fig. 1d**). We fit the heights of these untranscribed nucleosomes with a Gaussian function for each sample (different tip and deposition), and we shifted all these distributions so that the Gaussian peak of each one was at 3 nm (which is the height we got when imaging nucleosomes alone with high frequency tips). Finally, we shifted all the other nucleosome heights in that sample by exactly the same amount as the untranscribed nucleosomes. In general, this correction shift was between 0.2–0.8 nm for each sample, with the higher shifts for samples imaged with low-frequency tips.

Percentages of hexamers were calculated as the fraction of transcribed particles with heights under 2.4 nm. Amounts of bare DNA were estimated as the percentage of molecules without nucleosomes in the chased samples minus the corresponding percentage in the stalled samples.

Throughout this study, we used the length of free DNA (DNA not covered by protein) to estimate the position of the nucleosome on the template. Before Pol II passed the nucleosome, it covered part the upstream arm of the nucleosome; by contrast, after transcription, the upstream arm of the nucleosome was completely unobscured. Therefore, in order to obtain an accurate measurement of the length of the upstream arm of the nucleosome before transcription, we imaged a sample that lacked the polymerase but had a full-length template containing the nucleosome.

41. Kireeva, M.L., Lubkowska, L., Komissarova, N. & Kashlev, M. Assays and affinity purification of biotinylated and nonbiotinylated forms of double-tagged core RNA polymerase II from *Saccharomyces cerevisiae*. *Methods Enzymol.* **370**, 138–155 (2003).
42. Zhang, Y. *et al.* DNA translocation and loop formation mechanism of chromatin remodeling by SWI/SNF and RSC. *Mol. Cell* **24**, 559–568 (2006).
43. Thåström, A., Lowary, P.T. & Widom, J. Measurement of histone–DNA interaction free energy in nucleosomes. *Methods* **33**, 33–44 (2004).
44. Rivetti, C., Guthold, M. & Bustamante, C. Scanning force microscopy of DNA deposited onto mica: equilibration versus kinetic trapping studied by statistical polymer chain analysis. *J. Mol. Biol.* **264**, 919–932 (1996).

doi:10.1038/nsmb.2164